Applied Physics A (2020) 126:422
https://doi.org/10.1007/s00339-020-03604-4

Applied Physics A
Materials Science & Processing

Influence of aging on transformation characteristic and phase structure of a Cu–12.4Al–1.2Ti–1.2Ta shape memory alloy

Koksal Yildiz[1]

Received: 23 February 2020 / Accepted: 4 May 2020 / Published online: 15 May 2020

Abstract
The effect of aging on the properties of a Cu–12.4Al–1.2Ti–1.2Ta (wt.%) high-temperature SMA was investigated throughout SEM/EDS, XRD and DSC experiments. It was found that the transformation behavior, the thermal properties and the phase structure of the alloy remarkably changed with homogenization process performed at 900 °C for 20 min and then aging at 400 and 500 °C for 1 h. Structural and morphological investigations revealed that the homogenization process caused martensitic decomposition in the alloy and austenite phase domains remained. Afterward, with the effect of thermal aging, the amount of the austenite phase increased and the α-phase domains nucleated and grew in the alloy. At elevated aging temperature, the amounts of the austenite and the α-phases in the alloy considerably increased and martensitic morphology disappeared. As a result of these, the phase structure of the alloy affected its thermal behavior and led to exhibit irreversible one-stage martensitic transformation behavior.

Keywords Shape memory materials · Martensite · Degradation · Phase structure

1 Introduction

Cu-based shape memory alloys (SMAs) have always been of great interest due to their high thermal stability and low production cost [1]. The transformation temperatures of Cu-based SMAs can vary from -100 °C to 200 °C, depending on their composition and grain sizes. Among many different Cu-based SMAs, the Cu–Al–Ni alloy system is the most interesting SMA group because of its good thermal stability and high operating temperatures [2, 3]. Therefore, with advancing technology, SMAs with the transformation temperatures of above 130 °C are needed in many application areas, such as automotive, robotics and aerospace industries [4]. In general, SMAs, which have the transformation temperatures of above 120 °C, are termed as high-temperature SMA [5]. Although the transformation temperatures of Cu–Al–Ni alloys can exceed 120 °C, its high brittleness and low workability caused by its microstructural properties, i.e., polycrstallinity and large grain size, limit its application areas [6]. Therefore, in recent years, CuAl-based alloy systems, which exhibit high-temperature shape memory behavior in different atomic components, have been produced and the disadvantageous properties, which are obstacle to their application areas, have witnessed an attempt to be improved [4, 5, 7–10].

The aim of this study is to investigate the effects of thermal aging performed at 400 and 500 °C for 1 h on the morphological, structural and transformation characteristics of Cu–12.4Al–1.2Ti–1.2Ta (wt.%) alloy, which has high-temperature shape memory behavior. Generally, the thermal aging process applied at different temperatures and time durations can directly affect the microstructural atomic order, transformation temperatures and phase structure of the alloy [11, 12].

2 Experimental details

The Cu–12.4Al–1.2Ti–1.2Ta (wt.%) alloy was produced in an arc-melter furnace under vacuum by using high-purity Cu (99%, Aldrich), Al (≥ 99.5%, A. Aesar), Ti (99.7%, Aldrich) and Ta (99.9%, Aldrich) powders. For homogenization, the produced ingot was heat-treated in a furnace at 900 °C for 1 day. After that, small bulk pieces were cut from the ingot and then were homogenized again in a furnace at 900 °C for

✉ Koksal Yildiz
kyildiz@firat.edu.tr

[1] Department of Physics, Firat University, 23119 Elazig, Turkey

20 min in order to eliminate cutting strains in the samples and to achieve their betalization. Afterward, the samples were divided into three groups: While the first group, which was unaged, was labelled as CATT-0 sample, the second and the third groups, which were thermally aged at 400 and 500 °C for 1 h, were labelled as CATT-400 and CATT-500 samples, respectively. Microstructural and morphological properties of the alloy samples were investigated by means of scanning electron microscope (SEM, ZEISS EVO MA10) images equipped with energy-dispersive X-ray spectrometer (EDS) spectra. Structural and crystallographic properties of the alloy samples were examined by taking X-ray diffractometer (XRD, Bruker Discover D8) patterns using CuK_{α} radiation at room temperature between $2\theta = 20^{\circ}$–90°. Transformation temperatures of the alloy samples were determined by differential scanning calorimeter (DSC, SII Nanotechnology EXSTAR DSC 7000) measurements at scan rates of 10 °C/min during heating and cooling under nitrogen gas atmosphere.

3 Results and discussion

Changes in morphological and microstructural properties of the Cu–12.4Al–1.2Ti–1.2Ta (wt.%) alloy, which has gone through thermal aging, were examined by taking SEM images. Figure 1 presents the SEM images of the CATT-0, CATT-400 and CATT-500 samples. The microstructure of the CATT-0 sample consists of very large-sized grains and contains a large number of voids of different sizes and surface cracks (Fig. 1a, b). The rather large grain structure and the excessive void concentrations have a negative effect on the mechanical and transformation properties of the alloy [6, 13–16]. According to the SEM image in Fig. 1a, b, the main martensitic phase in the CATT-0 sample is 18R martensite with a needle-like zigzag morphology. However, in some regions of the CATT-0 sample, the 2H martensite phase with thick lath-like variant morphology was also observed, but the volume fraction of this martensitic phase was much lower than that of the 18R phase. Detailed SEM investigations demonstrated that the microstructure of the CATT-0 sample contains precipitate phases, which are rarely dispersed in the matrix and have less than 2 μm in sizes. EDS spectra revealed that chemical compositions of these precipitates marked by red and blue arrows in Fig. 1b are 75.49 at. % Cu + 24.46 at. % Al + 0.05 at. % Ti and 79.8 at. % Ta + 11.1 at. % Cu + 6.69 at. % Ti + 2.41 at. % Al, respectively. According to the EDS analysis performed, these precipitate phases are the austenite Cu_3Al (β-phase) and Ta-rich (β-Ta) phases. The results indicate that the microstructure of the CATT-0 sample includes the austenite phase at room temperature, as well as the 18R martensite phase. As previously mentioned in the experimental section, all of the samples examined in this study were heat-treated at 900 °C for 20 min in order to achieve betalization. To avoid the eutectoid decomposition reaction ($\beta \rightarrow \alpha + \gamma_2$) at 565 °C, the samples were quenched into room temperature water after the betalization process at high temperature. However, after the betalization process, it is obvious that a small amount of the austenite β-phase remained in the microstructure of the CATT-0 sample.

Figure 1c, d, which displays SEM images of the CATT-400 sample, indicates that the morphological properties of the Cu–12.4Al–1.2Ti–1.2Ta (wt.%) alloy changed as result of thermal aging applied at 400 °C for 1 h. As can be seen from Fig. 1c, the volume fractions of both the needle-like 18R martensite and the lath-like 2H martensite phases in the microstructure were increased. Furthermore, the equilibrium α-phase precipitated in the matrix of the CATT-400 sample. These α-phase colonies are clearly visible in the upper side of Fig. 1c, and in Fig. 1d, very dense α-phase colonies are observed in different regions of the sample. When the as-quenched alloy sample was heat-treated at the temperatures of above 350 °C and then quenched into room temperature, the α-phase nucleated and grew in its microstructure as a result of the complex phase transformation processes [17–20]. Cu-based SMAs have different phase transition behavior depending on aging temperatures and time durations. Chen et. al [12] reported that the aging at 500 °C for increasing time durations caused the phase transition sequence of $\beta \rightarrow \beta + B2 \rightarrow \beta + B2 + \alpha \rightarrow B2 + \alpha + \gamma_2$ in the Cu–14.1Al–9Ni (wt.%) alloy. As for the CATT-0 sample, with the effect of thermal aging at 400 °C for 1 h, the α-phase precipitated and coalesced in the matrix. Nevertheless, no other precipitate phases were observed.

SEM images of the CATT-500 sample shown in Fig. 1e, f indicate that the increasing aging temperature caused dramatic changes in the microstructure of the Cu–12.4Al–1.2Ti–1.2Ta (wt.%) alloy. It is obvious that the microstructure of the CATT-500 alloy sample contains a mixture of the austenite phase domains and the α-phase colonies that completely cover the matrix. It is well known that the aging carried out at higher temperatures than austenite finish temperature of the alloy leads to the formation of the austenite phase in the Cu-based SMAs [21]. Taking into account the SEM/EDS investigations of the CATT-0, the volume fraction of the austenite Cu_3Al phase, which remained after the betalization process, was increased with increasing aging temperature. Hereby, no martensite variants were observed on the SEM images of the CATT-500 sample, and a different precipitate phase was not detected either.

Figure 2 illustrates XRD patterns of CATT-0, CATT-400 and CATT-500 alloy samples taken at room temperature. The XRD pattern of the CATT-0 sample in Fig. 2a contains both the martensite and the austenite phase reflections. The austenite Cu_3Al phase peak at $2\theta \approx 31.88°$ agrees

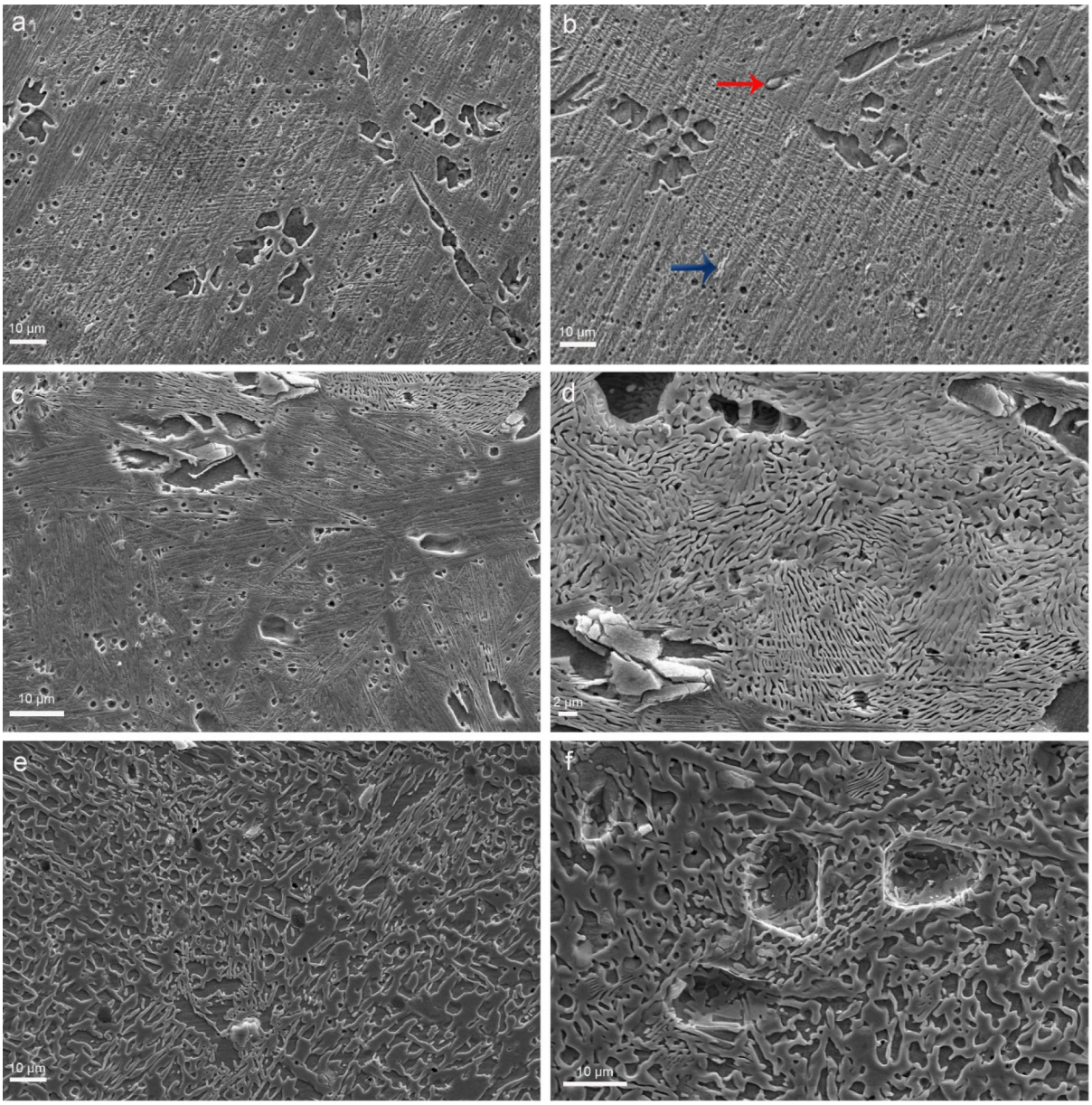

Fig. 1 SEM images of **a**-**b** CATT-0, **c**-**d** CATT-400 and **e**–**f** CATT-500 alloy samples

well with the SEM/EDS observations of the CATT-0 sample. This means that the ordering reaction ($B2 \rightarrow DO_3$) could not be suppressed during water quenching of the Cu–12.4Al–1.2Ti–1.2Ta (wt.%) alloy [22]. The XRD pattern in Fig. 2a also indicates that the amount of the austenite phase in the microstructure of the CATT-0 sample is relatively high, whereas that of Ta-rich (β-Ta) precipitate phase is too low to detect. The maximum intense diffraction peak in Fig. 2a is the reflection of (0018) at $2\theta \approx 42.87^{\circ}$, which was the characteristic reflection of 18R martensite phase. Although all martensite reflections in Fig. 2a are identified as the 18R, the pattern includes the 2H martensite phase as well. Otherwise, it is clear that many reflections of the 18R and the 2H martensite phases are overlapped in the XRD pattern where two martensite phases coexist due to their complicated monoclinic (18R) and orthorhombic (2H) crystal structures [23, 24]. Therefore, distinguishing and analyzing the superposing diffraction peaks of these two martensitic phases in XRD patterns are difficult.

The XRD pattern of the CATT-400 sample is plotted in Fig. 2b. The effect of thermal aging on the structural and crystallographic properties of the alloy is quite clear in Fig. 2b. The pattern is comprised of the martensite, the austenite and the α-phase reflections. This is in good accordance with the SEM/EDS observations of the CATT-400 sample in Fig. 1c, d. The XRD pattern of the CATT-500

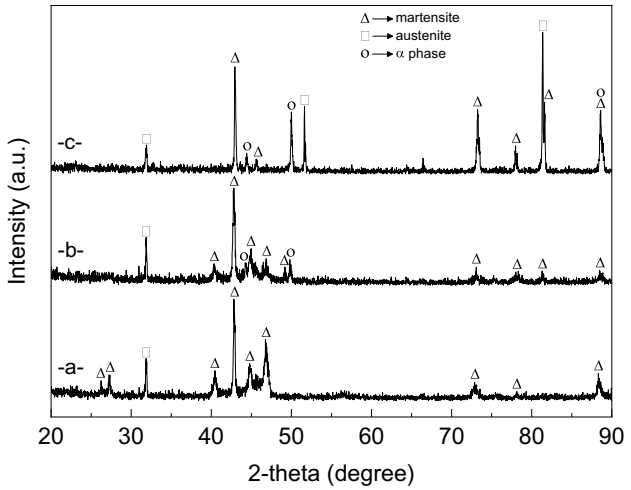

Fig. 2 XRD patterns of **a** CATT-0, **b** CATT-400 and **c** CATT-500 alloy samples taken at room temperature between $2\theta = 20^{\circ}$–90°

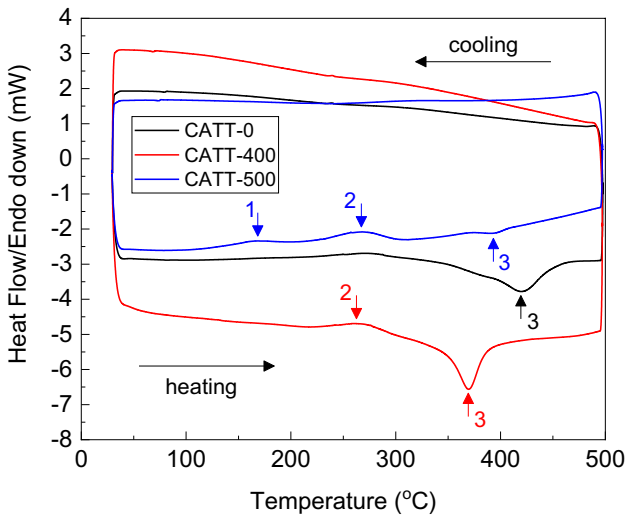

Fig. 3 DSC scans of **a** CATT-0, **b** CATT-400 and **c** CATT-500 alloy samples upon heating and cooling

sample is shown in Fig. 2c. In accordance with its SEM/EDS observations, the dramatic changes in the structural and crystallographic properties of the alloy thermally aged at 500 °C for 1 h are clearly shown in Fig. 2c. As a result of the thermal aging applied at 500 °C for 1 h, the numbers and the intensities of the austenite and the α-phase reflections increased considerably in Fig. 2c, which means that the higher aging temperatures are the higher volume fractions of the austenite and the α-phases in the microstructure of the Cu–12.4Al–1.2Ti–1.2Ta (wt.%) alloy.

The transformation properties of the CATT-0, CATT-400 and CATT-500 alloy samples were studied by performing DSC measurements between room temperature and 500 °C upon heating and cooling. All of the alloy samples were cycled twice during heating and cooling steps, and the second DSC cycles were used to determine martensitic transformation temperatures of the alloy samples. It is well known that the results obtained from a single DSC cycle in Cu-based SMAs can be misleading because the transformation peaks of the alloy can be observed at different temperature values rather than the temperature values that they should be due to quenched-in vacancy in the microstructure [25, 26]. As a result of the DSC measurements performed, the DSC curves shown in Fig. 3 were obtained for the samples. On the heating steps, while the CATT-0 sample has a rather broad endothermic transformation peak at 421.5 °C (peak 3), the CATT-400 sample exhibits a weak exothermic peak at 262.4 °C (peak 2) and a broad endothermic peak at 370.3 °C (peak 3). However, three peaks were observed in the DSC curve of the CATT-500 sample: two weak exothermic peaks at 168 °C (peak 1) and 265.1 °C (peak 2), respectively, and a weak endothermic transformation peak at 394.8 °C (peak 3). Consequently, it was revealed that the thermal aging process influenced the thermal behavior of the Cu–Al–Ti–Ta alloy.

The results obtained from the DSC curves on heating in Fig. 3 are quite compatible with the SEM/EDS and XRD results of the samples. It is thought that the peak 1 detected in only the DSC curve of the CATT-500 sample represents the ordering reaction of the α-phase in the microstructure of the sample [27]. Although the α-phase was detected in the microstructures of both CATT-400 and CATT-500 alloy samples, the peak 1 was not observed in the DSC curve of the CATT-400 sample. When the XRD patterns of the samples are examined in Fig. 2, it can be clearly seen that the intensities and numbers of diffraction peaks belonging to the α-phase shown in Fig. 2c are much higher than those in Fig. 2b. This may be an indication why the α-phase is not detected in the heating DSC curve of the CATT-400 sample because volume fraction of that phase in the CATT-400 sample is lower than that in the CATT-500 sample.

The exothermic peak 2 in the DSC curves of both CATT-400 and CATT-500 samples on heating is the peak of the ordering of the martensitic phase ($\beta' \rightarrow \beta'_1$) in their microstructures [28, 29]. Finally, the endothermic peak 3 in the DSC curves of all samples stands for the reverse (martensite to austenite) martensitic transformation. The DSC results of the samples on heating steps indicated that, with increasing aging temperature, significant changes were observed in both the energies and temperature values of the reverse transformation peaks of the samples. The lowest energy reverse transformation peak was observed in the CATT-500 sample. As the microstructure of the CATT-500 sample contains the austenite β-phase domains in the high volume fraction, the reverse transformation peak of the sample becomes quite weak. Simultaneously, the reverse transformation peak temperatures of the samples were shifted to the low-temperature region with the

effect of aging treatment. This is directly related to the quenched-in vacancy concentration in the microstructures of the samples since both the effect of the aging temperatures and the reduction in its concentration in the microstructure of the alloy can cause a decrease in the reverse transformation temperature [30].

In contrast with their heating DSC steps, none of the alloy samples have a forward (austenite to martensite) transformation peak on the cooling steps of the alloy samples, as can be seen in Fig. 3. This behavior is generally observed in Ti-based SMAs, where there are two hypothetical aspects causing this: The transformation enthalpy value between the austenite and martensite phase transformation is intrinsic low and/or partial transformations [31, 32]. However, similar behavior of Cu-based SMAs is quite unusual and has been observed in only a few studies in the literature [27, 33]. The increasing aging temperature and time duration lead to stabilization of the alloy, followed by martensitic degradation, which affects the reversible martensitic transformation characteristic of the alloy, causing it to exhibit irreversible transformation behavior [33]. Thus, the shape memory behavior of the alloy is eliminated resulting in the thermal aging treatments carried out at 900 °C for 20 min and at 400 and 500 °C for 1 h having a dramatic effect on the martensitic phase transformation behavior of the Cu–12.4Al–1.2Ti–1.2Ta (wt.%) alloy. Therefore, all alloy samples display irreversible martensitic transformation behavior with the effect of martensitic degradation. The reason of this martensitic degradation is yet unclear. On the other hand, the effects of the austenite phase at room temperature, the voids with different sizes, the cracks, the α-phase and also the defects in the microstructures of the alloy samples on the martensitic transformations should be examined in further detail, which means that additional new studies are needed.

Cu-based SMAs are very sensitive to both heat treatments, depending on which temperature and time duration are performed and cooling conditions to ambient temperature. Mentioned external stimulates have a great effect on their microstructural, crystallographic, transformation and mechanical properties [9, 11, 14, 30, 34, 35]. In previous work [36], it has been stated that the microstructure, the martensitic transformation behavior and shape memory properties of the Cu–12.4Al–1.2Ti–1.2Ta (wt.%) high-temperature shape memory alloy, which is heat-treated at 850 °C for 2.4 ks and then cooling to room temperature under different cooling conditions after its homogenization performed at 900 °C for 24 h, changed obviously. However, in this work, it can be clearly seen that the minor change in betalization temperature and time duration may considerably alter its phase components and transformation behavior in spite of having the same homogenization condition.

4 Conclusions

(1) The homogenization process for the betalization of the alloy samples performed at 900 °C for 20 min led to the martensite phase decomposition and the formation of the austenite phase at room temperature.

(2) When the alloy sample was aged at 400 °C for 1 h, the process of the martensitic decomposition proceeded and, therefore, the amount of the austenite phase in the microstructure increased. Then, the austenite phase transformed into the α-phase during the aging treatment. In the morphological investigation, the α-phase colonies were observed in the matrix, but no another precipitation phase was detected.

(3) With the effect of aging treatment at 500 °C for 1 h, it was deduced that the phase structure and the morphological properties of the alloy sample completely changed. Only, the austenite phase domains and the α-phase colonies were observed in the SEM observations of the alloy sample.

(4) With the change in the phase structure of the alloy, the transformation behavior of the alloy altered, as well. The results revealed that all the alloy samples, which were homogenized and then aged, exhibited irreversible martensitic transformation behavior because of the martensitic degradation. As a result, it is believed that this behavior may have a negative effect on the shape memory properties of the alloy samples.

Funding This research did not receive any specific grant from funding agencies in the public, commercial or not-for-profit sectors.

References

1. N. Suresh, U. Ramamurty, Aging response and its effect on the functional properties of Cu–Al–Ni shape memory alloys. J Alloy Compd **449**, 113–118 (2008). https://doi.org/10.1016/j.jallcom.2006.02.094
2. R.D. Cava, C. Bolfarini, C.S. Kiminami, E.M. Mazzer, W.J.B. Filho, P. Gargarella, J. Eckert, Spray forming of Cu–11.85Al–3.2Ni–3Mn (wt%) shape memory alloy. J Alloy Compd **615**, S02–606 (2014). https://doi.org/10.1016/j.jallcom.2013.11.166
3. Z.G. Wei, H.Y. Peng, W.H. Zou, D.Z. Yang, Aging effects in a Cu-12Al-5Ni-2Mn-1Ti shape memory alloy. Metall Mater Trans A **28**, 955–967 (1997). https://doi.org/10.1007/s11661-997-0226-z
4. T.N. Raju, V. Sampath, Effect of ternary addition of iron on shape memory characteristics of Cu-Al alloys. J Mater Eng Perform **20**, 767–770 (2011). https://doi.org/10.1007/s11665-011-9916-1
5. C.P. Wang, Y. Su, S.Y. Yang, Z. Shi, X.J. Liu, A new type of Cu–Al–Ta shape memory alloy with high martensitic transformation

temperature. Smart Mater Struct **23**, 025018 (2014). https://doi.org/10.1088/0964-1726/23/2/025018
6. K. Otsuka, C.M. Wayman, *Shape Memory Materials* (Cambridge University Press, Cambridge, 1998)
7. T.N. Raju, V. Sampath, Influence of aluminium and iron contents on the transformation temperatures of Cu-Al-Fe shape memory alloys. Trans IIM **64**, 165–168 (2011). https://doi.org/10.1007/s12666-011-0032-6
8. K. Yildiz, M. Kök, F. Dağdelen, Cobalt addition effects on martensitic transformation and microstructural properties of high-temperature Cu–Al–Fe shape-memory alloys. J Therm Anal Calorim **120**, 1227–1232 (2015). https://doi.org/10.1007/s10973-015-4395-5
9. K. Yildiz, E. Balci, S. Akpinar, Quenching media effects on martensitic transformation, thermodynamic and structural properties of Cu–Al–Fe–Ti high-temperature shape memory alloy. J Therm Anal Calorim **129**, 937–945 (2017). https://doi.org/10.1007/s10973-017-6219-2
10. J. Lelatko, H. Morawiec, High temperature Cu–Al–Nb-based shape memory alloys. J. Phys. IV France (2001). https://doi.org/10.1051/jp4:2001881
11. N. Kayali, S. Özgen, O. Adigüzel, Aging effects on ordering degree and morphology of 18R-type martensite in shape memory CuZnAl alloys. Mater Res Bull **32**, 569–578 (1997). https://doi.org/10.1016/S0025-5408(97)00024-X
12. C.H. Chen, C.C. Yang, T.F. Liu, Phase transition in a Cu-14.1Al-9.0Ni alloy. Mater Sci Eng A **354**, 377–386 (2003). https://doi.org/10.1016/S0921-5093(03)00041-8
13. J.S. Lee, C.M. Wayman, Grain refinement of a Cu-Al-Ni shape memory alloy by Ti and Zr additions. Trans JIM **27**, 584–591 (1986). https://doi.org/10.2320/matertrans1960.27.584
14. U. Sari, T. Kirindi, F. Ozcan, M. Dikici, Effects of aging on the microstructure of a Cu–Al–Ni–Mn shape memory alloy. Int J Miner Metall Mater **18**, 430–436 (2011). https://doi.org/10.1007/s12613-011-0458-1
15. X. Zhang, Q.-S. Liu, Influence of alloying element addition on Cu–Al–Ni high temperature shape memory alloy without second phase formation. Acta Metall Sin (Engl. Lett.) **29**, 884–888 (2016). https://doi.org/10.1007/s40195-016-0467-1
16. G.N. Sure, L.C. Brown, The mechanical properties of grain refined β-CuAlNi strain-memory alloys. Metall Trans A **15A**, 1613–1621 (1984). https://doi.org/10.1007/BF02657801
17. C.H. Chen, T.F. Liu, Phase transformations in a Cu-14.2Al-7.8Ni alloy. Metall Mater Trans A **34A**, 503–509 (2003). https://doi.org/10.1007/s11661-003-0086-0
18. J. Singh, H. Chen, C.M. Wayman, Precipitation behavior of a Cu–Al–Ni shape memory alloy at elevated temperatures. Scr Metall **19**, 231–234 (1985). https://doi.org/10.1016/0036-9748(85)90188-7
19. J. Singh, H. Chen, C.M. Wayman, Transformation sequence in a Cu-Al-Ni shape memory alloy at elevated temperatures. Metall Trans A **17A**, 65–72 (1986). https://doi.org/10.1007/BF02644443
20. M. Bouabdallah, G. Baguenane-Benalia, A. Saadi, H. Cheniti, J.C. Gachon, E. Patoor, Precipitation sequence during aging in β_1 phase of Cu–Al–Ni shape memory alloy. J Therm Anal Calorim **112**, 279–283 (2013). https://doi.org/10.1007/s10973-012-2837-x
21. F.R. Milhorato, E.M. Mazzer, Effects of aging on a spray-formed Cu–Al–Ni–Mn–Nb high temperature shape memory alloy. Mater Sci Eng A **753**, 232–237 (2019). https://doi.org/10.1016/j.msea.2019.03.024
22. V. Asanović, K. Delijić, The mechanical behavior and shape memory recovery of Cu–Zn–Al alloys. Metalurgija **13**, 59–64 (2007)
23. E.M. Mazzer, P. Gargarella, R.D. Cava, C. Bolfarini, M. Galano, C.S. Kiminami, Effects of dislocations and residual stresses on the martensitic transformation of Cu–Al–Ni–Mn shape memory alloy powders. J Alloy Compd **723**, 841–849 (2017). https://doi.org/10.1016/j.jallcom.2017.06.312
24. M. Şaşmaz, A. Bayri, Y. Aydoğdu, The magnetic behavior and physical characterization of Cu–Mn–Al ferromagnetic shape memory alloy. J Supercond Nov Magn **24**, 757–762 (2011). https://doi.org/10.1007/s10948-010-0934-2
25. E.M. Mazzer, C.S. Kiminami, C. Bolfarini, R.D. Cava, W.J. Botta, P. Gargarella, Thermodynamic analysis of the effect of annealing on the thermal stability of a Cu–Al–Ni–Mn shape memory alloy. Thermochim Acta **608**, 1–6 (2015). https://doi.org/10.1016/j.tca.2015.03.024
26. K. Yildiz, Oxidation of high-temperature Cu–Al–Fe shape memory alloy. J Therm Anal Calorim **123**, 409–412 (2016). https://doi.org/10.1007/s10973-015-4912-6
27. A.T. Adorno, M.R. Guerreiro, A.V. Benedetti, Thermal behavior of Cu-Al alloys near the α-Cu–Al solubility limit. J Therm Anal Calorim **65**, 221–229 (2001). https://doi.org/10.1023/A:1011549223427
28. A.T. Adorno, R.A.G. Silva, Effect of Ag additions on the reverse martensitic transformation in the Cu-10 mass% Al alloy. J Therm Anal Calorim **83**, 241–246 (2006). https://doi.org/10.1007/s10973-005-6986-z
29. A.T. Adorno, R.A.G. Silva, Aging behavior in the Cu-10wt.%Al and Cu-10wt.%Al-4wt.%Ag alloys. J Alloy Compd **473**, 139–144 (2009). https://doi.org/10.1016/j.jallcom.2008.05.072
30. Z. Jiao, Q. Wang, F. Yin, C. Cui, Effect of precipitation during parent phase aging on the microstructure and properties of a refined CuAlMn shape memory alloy. Mater Sci Eng A **737**, 124–131 (2018). https://doi.org/10.1016/j.msea.2018.09.037
31. Y. Cui, Y. Li, K. Luo, H. Xu, Microstructure and shape memory effect of Ti-20Zr-10Nb alloy. Mater Sci Eng A **527**, 652–656 (2010). https://doi.org/10.1016/j.msea.2009.08.063
32. P. Xue, Y. Li, F. Zhang, C. Zhou, Shape memory effect and phase transformations of Ti-19.5Zr-10Nb-0.5Fe alloy. Scr Mater **101**, 99–102 (2015). https://doi.org/10.1016/j.scriptamat.2015.02.003
33. V. Pelosin, A. Rivière, Structural and mechanical spectroscopy study of the β1′ martensite decomposition in Cu-12% Al-3% Ni(wt.%) alloy. J Alloy Compd **268**, 166–172 (1998). https://doi.org/10.1016/S0925-8388(97)00595-1
34. M. Eskil, N. Kayali, X-ray analysis of some shape memory CuZnAl alloys due to the cooling rate effect. Mater Lett **60**, 630–634 (2006). https://doi.org/10.1016/j.matlet.2005.09.019
35. E. Obradó, L1. Mañosa, A. Planes, R. Romero, A. Somoza, Quenching effects in Cu-Al-Mn shape memory alloy. Mater Sci Eng A **273**, 586–589 (1999). https://doi.org/10.1016/S0921-5093(99)00434-7
36. K. Yildiz, On the influence of cooling rate in heat-treated Cu–Al–Ti–Ta high-temperature shape memory alloys. Mater Sci Eng A **773**, 138860 (2020). https://doi.org/10.1016/j.msea.2019.138860